



A comparison of molecular dynamic simulations and experimental observations: the sputtering of gold {1 0 0} by 20 keV argon

C.M. McQuaw^{*}, E.J. Smiley, B.J. Garrison, N. Winograd

*Department of Chemistry, The Pennsylvania State University, 184 Materials Research Institute Building,
University Park, PA 16802, USA*

Available online 24 May 2004

Abstract

In order to further illuminate the sputtering process, the bombardment of Au {1 0 0} by 20 keV Ar is investigated using molecular dynamics (MD) simulations. The MD results are compared to experimental observations discussed by M.W. Thompson in his recent review of the atomic collision cascade process [Vacuum 66 (2) (2002) 99]. In his review, Thompson explains characteristics of experimental time-of-flight (ToF) and polar distributions using ejection mechanisms. Using mechanisms deduced from the MD results the ToF distributions are divided at 70 μ s with atoms sputtered by direct recoil at shorter ToF and atoms sputtered by focused collision sequences at longer ToF. Surface lens assisted focusing arises from impacts along crystal symmetry lines (slice impact points) and results in a peak at surface normal in the polar distribution. These conclusions help to clarify the experimental observations made by Thompson and contribute to the overall description of sputtering.

© 2004 Elsevier B.V. All rights reserved.

Keywords: Molecular dynamics; Time-of-flight; Ejection mechanism; Sputtering

1. Introduction

A fundamental understanding of the events that lead to sputtering is valuable in explaining experimental results. Presented here is an investigation into the mechanisms involved in the sputtering of Au {1 0 0} by 20 keV Ar using molecular dynamics simulations. The recent article by Thompson that discusses collision cascades [1] inspired this work. The results of this investigation are compared to his experimental results in order to emphasize the pre-

dictive and elucidative power of molecular dynamics (MD) simulations.

2. Experimental

The experimental method used by Thompson has been extensively described elsewhere [1–3] and, therefore, is only briefly explained here. A pulsed mass-separated 20 keV argon ion beam is used to bombard a radioactive gold (1 0 0) crystal along the [1 1 0] direction 45° from surface normal. A fraction of the sputtered atoms travel through a collimator down a flight path to a spinning cylinder while a majority of the sputtered atoms impinge the static

^{*} Corresponding author. Tel.: +1-814-865-0493;

fax: +1-814-863-0618.

E-mail address: cmm336@psu.edu (C.M. McQuaw).

cylindrical collector surrounding the sample stage. The sputtering yield is determined by autoradiography densitometry from the photographic film lining the cylinders.

3. Simulation

Only a brief description of the molecular dynamics method used is outlined here as it has been given previously [4]. For the simulations a Au {1 0 0} surface is approximated by 42,135 atoms arranged in 30 layers of 2809 atoms each. The crystal size is selected to match the energy and angular distributions of a larger crystal. The atoms have zero initial kinetic energy and are initially located in their bulk equilibrium positions. The “molecular dynamics and Monte Carlo-corrected effective medium” (MD/MC-CEM) potential [5,6] is used for the interaction potential of Au.

Each trajectory begins when an Ar atom with 20 keV of kinetic energy bombards the surface at 45° from surface normal. A Molière potential is used to describe Ar–Au interactions. Open boundary conditions are used because any particle leaving the side or bottom of the simulation crystal would penetrate deeper into a larger crystal. The calculation is ended when the most energetic particle in the solid lacks the energy to overcome its attractive interactions to the solid. At the end of a trajectory the sputtered atoms have traveled tens of Angstroms, whereas, in the experiment the atoms have traveled tens of centimeters. For the simulation data the time for a sputtered atom to travel the experimental flight path is extrapolated using the atom’s final position, velocity, and time.

The calculations are performed for 750 impact points at randomly selected positions within the impact zone (see Fig. 1A). Many impact points are required because the experimental data are an average over a multitude of Ar impacts on the surface. The impact zone is reduced to a rectangle near the center of the crystal because the surface has translational and rotational symmetries.

At each timestep, the Molière interaction between pairs of atoms is calculated and if the interaction is greater than 5 eV the event is defined as a collision. Upon completion of a trajectory, mechanisms are

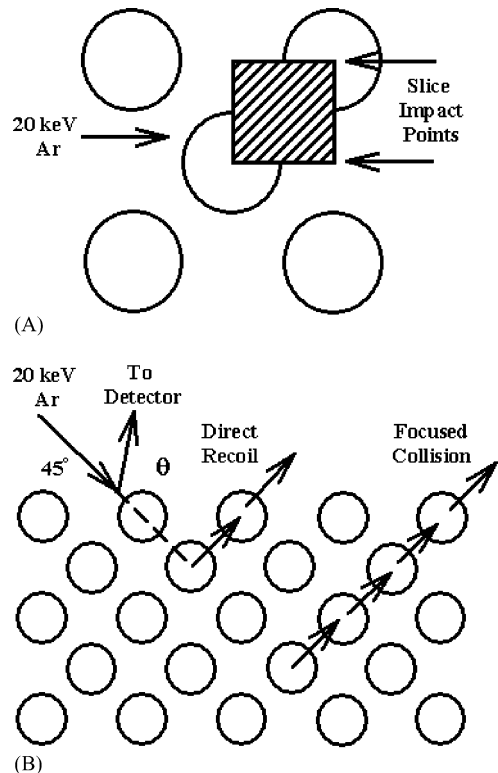


Fig. 1. (A) Top view of Au {1 0 0} surface with the circles representing Au atoms and the square showing the impact zone. Slice impact points are impact points directly on a crystal row. (B) Side view with circles representing Au atoms and arrows indicating the direction of atom motion. Two different ejection mechanisms are illustrated: direct recoil and focused collision sequences. The detection angle, θ , is defined by the direction of the incoming Ar atom (dashed line) and the position of the detector.

defined by following the energy of the collision cascade. An ejected atom of interest is selected and the collisions involving this atom are followed backwards through time. When the first collision involving said atom is found the atom that collides with it is selected. This atom is then followed backwards through time until its first collision. The process is continued similarly for several iterations. These points where the energy is transferred are used to define ejection mechanisms.

4. Results and discussion

The goal of this work is to carry out a mechanistic study of ejection processes as a function of

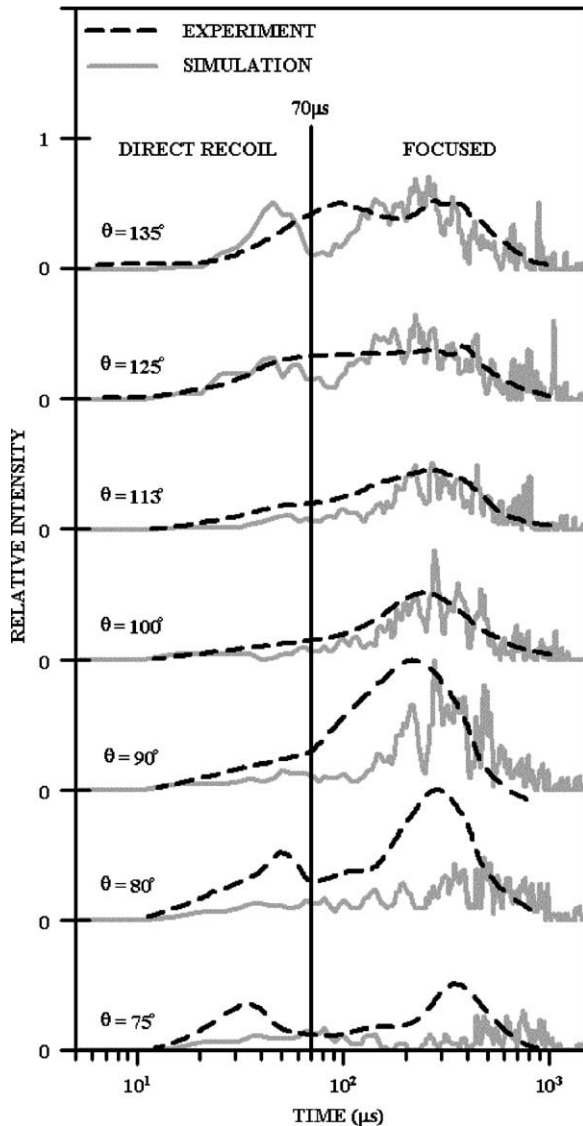


Fig. 2. Angularly resolved time-of-flight distributions of the experimental and simulation results. The experimental data are normalized to the maximum peak at $\theta = 90^\circ$, and the simulation data are normalized to the maximum peak at $\theta = 90^\circ$. A line at $70 \mu\text{s}$ is drawn to divide the spectra into major mechanistic contributors.

time-of-flight (TOF) and detection angle. Angularly resolved TOF distributions are presented as log-linear plots in Fig. 2 with the axes shifted vertically to separate the data. The major features of the experimental results are reproduced in the MD data although

Table 1

The percentage of the total yield at a given detector angle due to a specific mechanism

Mechanism	Angular percentage of total yield						
	135°	125°	113°	100°	90°	80°	75°
Direct recoil	10	21	9	17	0	7	21
Focused	57	58	52	51	42	15	12
Undetermined	33	21	39	32	58	78	67

The detection angle, θ , is defined in Fig. 1B.

the agreement is not perfect. The mechanism results are shown in Table 1. When an atom of interest lacks a collision record the mechanism is labeled as undetermined. An atom that is sputtered but lacks a collision record is involved in collisions with Molière interactions of less than 5 eV and many such collisions would be required for ejection. These sputtering events are part of a complex collision cascade and are traditionally known as ‘random’. A larger percent of undetermined mechanisms appear for the time-of-flight spectra at small angles and is probably a result of scattering within the crystal.

If an atom’s last three or fewer energy giving collisions involves the bombarding Ar atom then its ejection mechanism is termed ‘direct recoil’ (see Fig. 1B). Ejection by direct recoil leads to higher velocity atoms and is responsible for the peaks near $40 \mu\text{s}$ in the $\theta = 75^\circ$ and $\theta = 80^\circ$ spectra. This feature is in agreement with the mechanisms postulated by Thompson [1]. The MD results appear with a much lower intensity, because trajectories producing direct recoil have smaller yields and more impact points are required. The fast peak in the $\theta = 135^\circ$ spectrum is partially due to direct recoil, but is an aberration due to the large detection slit width required for analysis of simulation data (9.7° versus Thompson’s $<1^\circ$).

The majority of atoms that give rise to the spectra in Fig. 2 are sputtered by focused collisions. When collisions travel along crystal rows, transporting mainly only energy, they are termed ‘focused’ collisions. One such focused collision sequence is illustrated in Fig. 1B. This mechanism is 30% or more of the focused collisions at each detection angle. The focused collision sequence shown in Fig. 1B is especially prominent at $300 \mu\text{s}$ in the $\theta = 90^\circ$ spectrum. This mechanism is 80% of all focused ejections at this

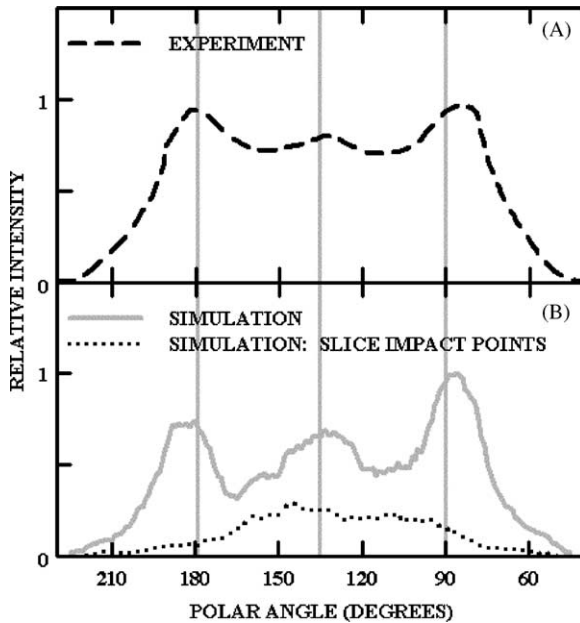


Fig. 3. Polar distributions. The polar angle, θ , is defined in Fig. 1B. (A) Experiment. (B) Simulation total yield and yield from slice impact points.

peak. Thompson interprets the major peak at longer ToF for larger detection angle as due mainly to focused collision sequences [1]. The MD results presented here agree with this interpretation.

The experimental and simulation polar distributions are given in Fig. 3. The yield agreement between the MD results and experiment is quite good. In ref. [1], Thompson attributes the $\theta = 135^\circ$ peak in the polar distribution (see Fig. 3A) to an ejection mechanism he defines as ‘assisted focusing by a surface lens.’ In this mechanism, four atoms at the surface form a ring, or a ‘lens,’ that an atom departs through, thus, guiding the direction and energy of the ejected atom. As seen in Fig. 3B, specific impact points—slice impact points (illustrated in Fig. 1A)—result in the surface normal peak in the simulation polar distribution. Slice impact points strike the crystal in the (1 0 0) plane that is normal to the surface and result in unique sputtering events. These impact points have been termed ‘slice’ because the sputtered atoms originate entirely from the same crystal plane as the impact point and appear as a slice of sputtered atoms. This

action results in two planes of relatively stationary atoms surrounding the departing atoms. These rows of stationary atoms act as surface lenses and guide the sputtering atoms. The surface lens action predicted by Thompson is largely due to slice impact points.

This mechanistic study focuses on the effects of large energy transferring collisions and does not elucidate the influence of lower energy collisions. Every collision affects the velocity and direction of the colliding atoms. The mechanisms described here help to explain the major features of polar and time-of-flight distributions.

5. Summary and conclusions

The collision cascade and mechanisms of sputtering were discussed for the bombardment of Au {1 0 0} by 20 keV Ar. Molecular dynamics simulations and experimental results were compared. The agreement between simulation and experimental polar and time-of-flight distributions is respectable. Direct recoil is the prominent mechanism of ejection for short ToF and smaller detection angles. Focused collision sequences similar to those described by Thompson [1] are the source of the main peak at longer ToF for larger detection angles. Slice impact points produce sputtering via surface lens assisted focusing and are responsible for the $\theta = 135^\circ$ peak in polar distributions of Au {1 0 0}. These results promote the use of MD as an approach for predicting and explaining the bombardment of solids by high energy projectiles.

Acknowledgements

Financial support from the National Science Foundation is gratefully acknowledged. The Academic Services and Emerging Technologies group at Pennsylvania State University provided us early access to the LION-XL PC cluster, thus, increasing our computational prowess. The authors wish to thank Chad Meserole, Zbigniew Postawa, James Watney, and Igor Wojciechowski for valuable discussions. We would also like to express our appreciation for the challenge posed by Sir Michael W. Thompson in Zvenigorod.

References

- [1] M.W. Thompson, *Vacuum* 66 (2) (2002) 99.
- [2] M.W. Thompson, B.W. Farmery, P.A. Newson, *Phil. Mag.* 18 (152) (1968) 361.
- [3] M.W. Thompson, *Nucl. Inst. Methods B* 18 (1987) 411.
- [4] B.J. Garrison, *Chem. Soc. Rev.* 21 (1992) 155.
- [5] M.S. Stave, D.E. Sanders, T.J. Raeker, A.E. DePristo, *J. Chem. Phys.* 93 (1990) 4413.
- [6] T.J. Raeker, A.E. DePristo, *Int. Rev. Phys. Chem.* 10 (1991) 1.